Poloidally asymmetric distribution of impurities in Joint European Torus plasmas

H. Chen, N. C. Hawkes, L. C. Ingesson, M. von Hellermann, K.-D. Zastrow et al.

Related Articles

High-performance double-filter soft x-ray diagnostic for measurement of electron temperature structure and dynamics
Rev. Sci. Instrum. 83, 10E129 (2012)

Molybdenum emission from impurity-induced m = 1 snake-modes on the Alcator C-Mod tokamak
Rev. Sci. Instrum. 83, 10E517 (2012)

Extreme ultraviolet spectroscopy and modeling of Cu on the SSPX Spheromak and laser plasma "Sparky"
Rev. Sci. Instrum. 83, 10E101 (2012)

Note: Measurement of the runaway electrons in the J-TEXT tokamak
Rev. Sci. Instrum. 83, 056108 (2012)

Effect of poloidal asymmetries on impurity peaking in tokamaks
Phys. Plasmas 19, 052307 (2012)
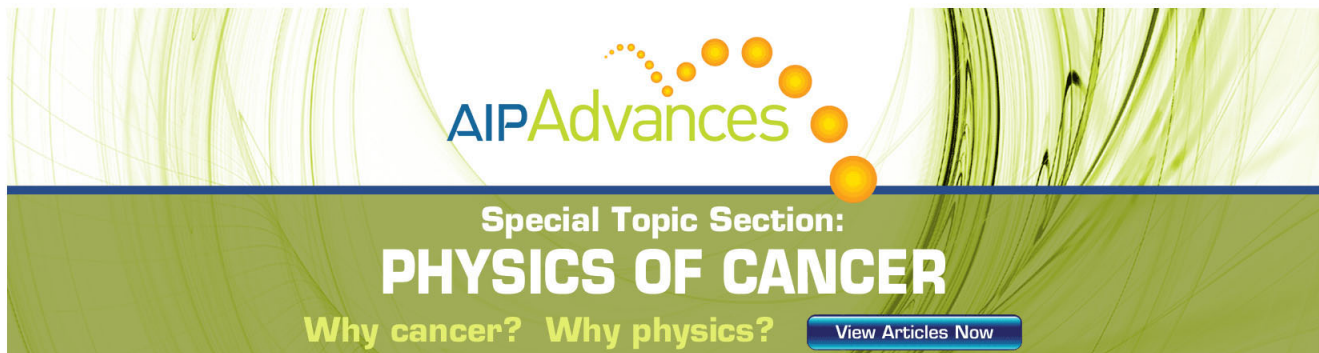
Additional information on Phys. Plasmas

Journal Homepage: http://pop.aip.org/

Journal Information: http://pop.aip.org/about/about_the_journal

Top downloads: http://pop.aip.org/features/most_downloaded

Information for Authors: http://pop.aip.org/authors

Poloidally asymmetric distribution of impurities in Joint European Torus plasmas

H. Chen[a)]
Imperial College, The Blackett Laboratory, London, SW7 2BZ, United Kingdom

N. C. Hawkes
UKAEA/Euratom, Fusion Association, Culham Science Centre, Abingdon, Oxon, OX14 3DB, United Kingdom

L. C. Ingesson, M. von Hellermann, and K.-D. Zastrow
Joint European Torus, Joint Undertaking, Abingdon, Oxon, OX14 3EA, United Kingdom

M. G. Haines, M. Romanelli,[b)] and N. J. Peacock
Imperial College, The Blackett Laboratory, London, SW7 2BZ, United Kingdom

Poloidally asymmetric distributions of nickel ions have been observed experimentally in Joint European Torus optimized shear tokamak plasmas following nickel laser injection experiments. Two types of asymmetries occur. In the first type of asymmetry, which has earlier been observed in high-confinement mode plasmas, nickel ions accumulate on the outboard side of the poloidal cross section. This can be explained well by fast toroidal plasma rotation driven by neutral beam injection. The second type of asymmetry was opposite in position: In a radio frequency heated optimized shear plasma, nickel ions have been seen to accumulate on the inboard side of the poloidal cross section. © *2000 American Institute of Physics.* [S1070-664X(00)01611-6]

I. INTRODUCTION

Poloidal asymmetries of particles in tokamak plasmas have been discussed theoretically for the cases of toroidal rotational plasma.[1–4] The effect of the rotation on impurity distribution has also been dealt with[5–7] based on the experimental results. Rozhansky and Tendler have presented an extensive review[8] on the effect of plasma rotation in tokamaks. The role of plasma rotations on the transitions to improved confinement regimes has been reviewed[9] in particular. Previously, in–out asymmetries have been observed in the Axially Symmetric Divertor Experiment (ASDEX)[10] and ASDEX-Upgrade,[11] and in Joint European Torus (JET) hot-ion high-confinement mode (*H*-mode) plasmas.[12,13]

In this paper, we report on the observation of in–out poloidal asymmetries of injected test ions in optimized shear (OS) plasmas in JET[14] following metal ion injection. Both asymmetries with the ion peak on the inboard and outboard of the plasma are seen. The asymmetric emission distribution from light impurities will be discussed. It should be noted that a slight up–down poloidal asymmetry of impurity was shown in JET[15] but will not be covered in this paper. The observed up–down asymmetry has so far not been explained by the models used for the strong up–down asymmetry observed in other tokamaks, such as Alcator-A[16] and Poloidal Divertor Experiment.[17]

II. IN–OUT ASYMMETRY IN PLASMAS WITH FAST TOROIDAL ROTATION

The OS discharges we analyzed, in which the asymmetries were observed, have about 17 MW neutral beam heating power and 6 MW rf heating power. See Fig. 1 for the main parameters of discharge 40551 in which the ion asymmetry was best shown. The plasma has a low-confinement mode edge condition as indicated by the D_α character. The internal transport barrier has $\nabla Ti/Ti \sim 25\,\mathrm{m}^{-1}$. The time of nickel injection is at 6.206 s, as shown in the Ni XXV line emission measurement. The rise of the Ni line emission in later time results from the extra Ni sources produced from the plasma–wall interaction during the edge localized mode (ELM) period. The ion temperature in the center of the plasma nearly reached 40 keV and the toroidal rotation speed of He-like nickel ions is up to $\sim 8 \times 10^5$ m/s.

The soft x-ray emission of Ni ions was analyzed by applying a tomographic reconstruction technique[18] onto the measurements of the soft x-ray camera system. The background soft x-ray emission increases approximately linearly in time prior to injection, due to the slow increase of electron density and temperature. Therefore, a linear fit to the background, extrapolated to the time of injection, is subtracted from the local emissivities. Figure 2 shows background subtracted reconstructed images; it can be seen that there is a strongly asymmetric emission distribution developing with time. At 514 ms after the injection of nickel, the ratio of the out–in emission peak is about 4 through the magnetic axis.

When there is a toroidal momentum input, such as is the case when using unbalanced tangential neutral beam injec-
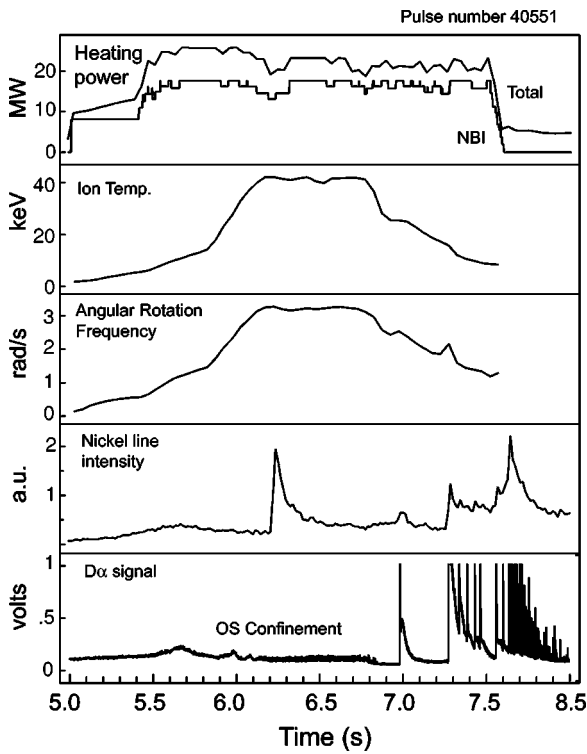
FIG. 1. An overview of an OS discharge. Nickel was injected at 6.206 s.

dition for the impurity ion distribution n_I, as a function of minor radius r and poloidal angle θ for a fast toroidally rotating plasma is described as[7]

$$n_I(r) = n_I|_{r=0} \left(\frac{n_i(r)}{n_i(0)} \right)^{z_I/z_i}$$

$$\times \exp\left[\frac{\Omega^2}{2T} M \left(1 - \frac{m}{M} \frac{Z_I T_e}{T + Z_i T_e} \right) (R^2 - R_0^2) \right]$$

$$\times \exp\left[-\frac{\Omega^2}{2} \frac{Z_I}{Z_i} \frac{m}{T + Z_i T_e} (r^2 + 2rR_0) \right].$$

where the subscripts I, i, and e stand for impurity ions, main ions, and electron, respectively.

The ion temperature and toroidal rotation profiles, as measured by charge–exchange diagnostics using fully stripped carbon ions, are shown in Fig. 3 for the discharge with the strong asymmetry of nickel emission. The ion temperature and the toroidal rotation of nickel measured by a high resolution x-ray crystal spectrometer are shown as crosses in Fig. 3 at $r/a \sim 0.3$. It has a radial error bar of ± 0.15 m for this discharge. This measurement has a good consistency with the measurements of charge–exchange diagnostics. Therefore we assume the ion temperature to be the same for carbon and nickel ions. Given these plasma conditions, the predicted distribution of nickel ions from the above-given equation is shown in Fig. 4. The calculated value is vertically scaled to that derived from the tomographic reconstruction. There is a good agreement in the shape of the ion density between the calculation and the experimental values.

tion (NBI) as an auxiliary heating, the impurity ions can rotate supersonically in the toroidal direction ($v_\phi^I \geq v_{thermal}^I$), i.e., the ratio of ion toroidal rotation and thermal velocities (Mach number) exceeds one. The equilibrium con-
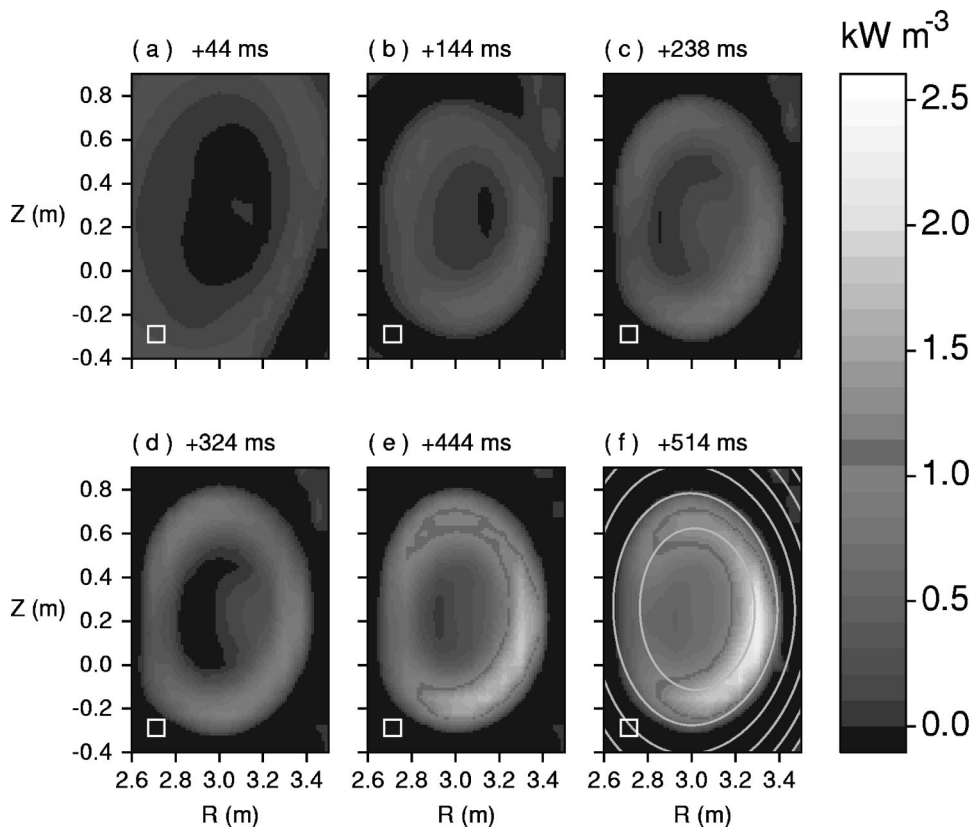

FIG. 2. The background-subtracted emission images from the soft x-ray tomographic reconstruction. The times given are relative to the injection time.
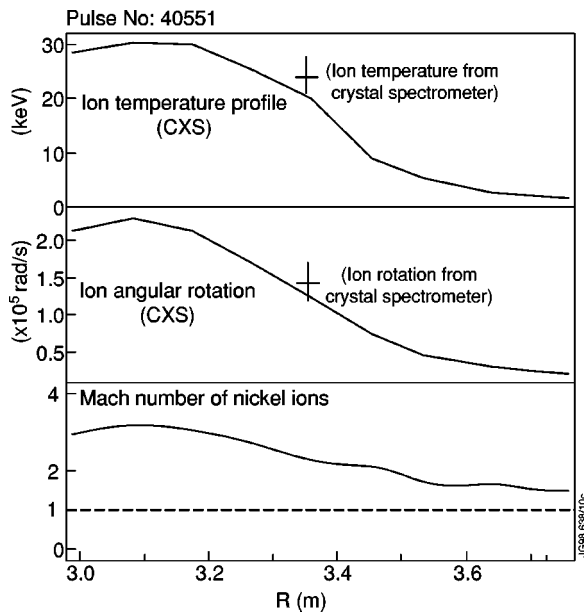
FIG. 3. Ion temperature and angular rotation profile measured by charge–exchange diagnostics for carbon ions. The measurements show good consistency with the crystal spectrometer measurement of nickel ions, shown as crosses. The Mach number of nickel ions is well above 1 across most of the plasma radius.

FIG. 5. Hollow carbon density and concentration profiles and the electron density profile in a typical JET H-mode plasma. The two lines indicate the positions R_1 and R_2, where the ratio of the carbon density and concentration are taken in the analysis.

III. HOLLOW DENSITY PROFILE OF LIGHT IMPURITIES

In JET high-confinement plasmas, light impurity concentration profiles [measured by charge–exchange spectrometers (CXS)] are commonly hollow. The features of the hollowness of carbon, neon, and nitrogen are similar and do not appear to be dependent on the impurity influx and content.[19] Because of the presence of the strong unbalanced neutral beam injection in these discharges, toroidal plasma rotation is high. Thus we investigated the interrelation between plasma toroidal rotation and hollowness of the light impurity profile.
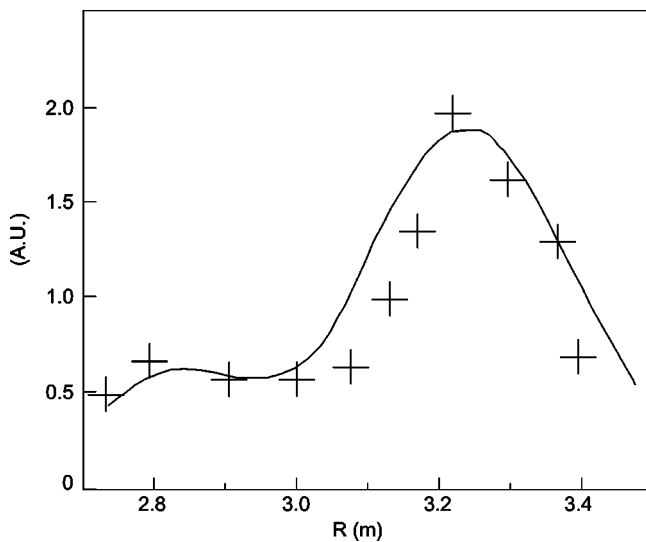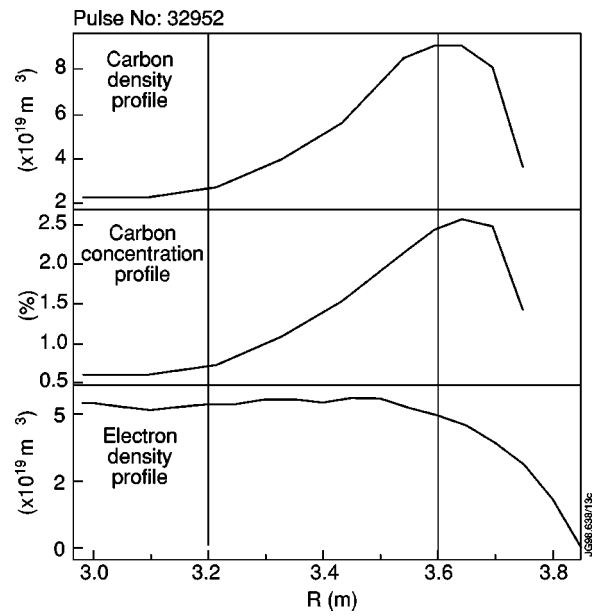
To investigate the correlation of the development of the hollow impurity density profile and the toroidal rotation, a simple analysis for an equilibrium plasma condition has been carried out. A number of H-mode discharges have been selected which have similar plasma parameters. We took the ratio (define as hollowness) of the carbon concentration (n_c) at two radial positions (shown in Fig. 5, $R_1 = 3.2$ m, $R_2 = 3.6$ m). Ratio $R = n_c(R_2)/n_c(R_1)$ was plotted against the maximum plasma toroidal rotation frequency, W (rad/s). Figure 6 shows the result of a typical pulse having both ELM-

FIG. 4. Ni density derived from the soft x-ray emissivity at $t = 6.72$ s (cross) and calculated Ni density at the same time (line).
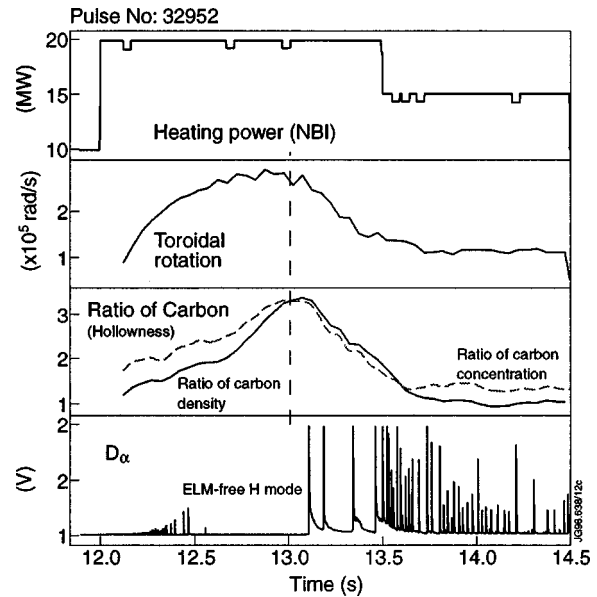
FIG. 6. The time history of the heating, toroidal rotation, and the hollowness of carbon density together with the edge condition of a H-mode plasma.
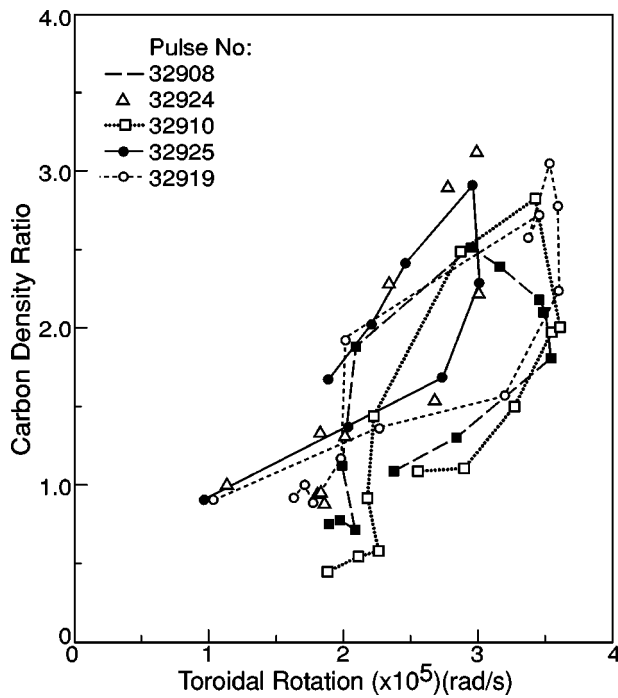
FIG. 7. The hollowness of the carbon profiles against the toroidal rotation in a number of discharges.

FIG. 8. The poloidally asymmetric emission from mostly light impurities.

free and ELMy phases. The evolution of hollowness in the discharge follows the increase and decrease of the toroidal rotation.

Plotting the hollowness against Ω for a number of discharges in Fig. 7, there appears to be an interdependence of these two parameters: The faster the plasma rotates, the hollower the carbon becomes. If the ion distribution were strongly affected by the toroidal plasma rotation, the asymmetric distribution of the density profile in the midplane would have a hollow profile. In JET the in–out asymmetry has been observed in a high confinement discharge.[15] In Fig. 8 the tomographic image is of the soft x-ray emission that comes mainly from carbon and other light impurities judging by the spectroscopic measurements. The emission, which is proportional to the impurity density, becomes progressively peaked off-axis following the increase of the toroidal rotation velocity. Note that the Mach numbers of carbon, neon, and chlorine all exceed one. This indicates that toroidal rotation could be one of the driving mechanisms for the hollow carbon profiles.

IV. ASYMMETRIC DISTRIBUTION OF IMPURITY IN RADIO FREQUENCY HEATING ONLY PLASMAS

An in–out poloidal asymmetry of the impurity distribution has been observed in a plasma (pulse 40051) with rf heating only in an optimized shear experiment. The rf heating power was 3 MW. The asymmetry is reversed in comparison with the asymmetry due to the unbalanced neutral beam heating.

An asymmetry of tomographic reconstructed nickel soft x-ray emission was observed during nickel injection experiments. Nickel was injected at 6.405 s. The electron temperature and density profiles in this discharge do not change ap-
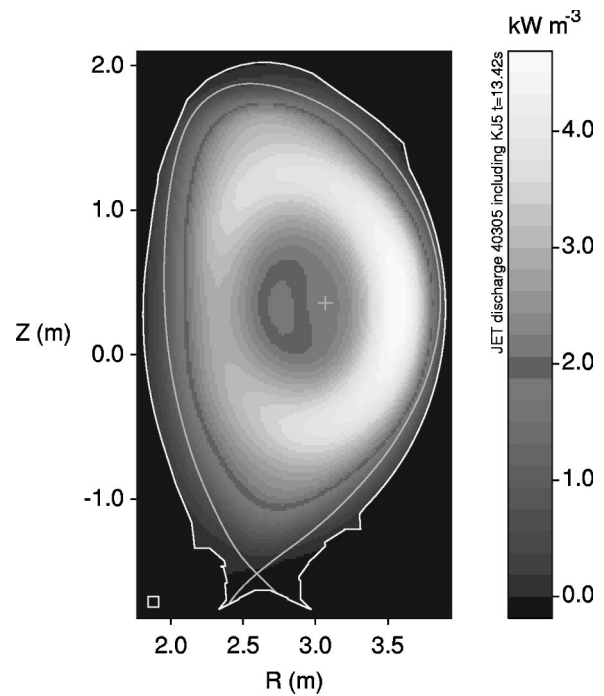
preciably in the time period of residence of nickel ions in the plasma, and thus a constant background was subtracted. The background-subtracted radiation measured by soft x-ray cameras is identified from the spectra of the soft x-ray pulse-height analyzer as line radiation from helium-like nickel. An asymmetry in the background-subtracted reconstructed soft x-ray emission is shown in Fig. 9 for 6.440 s. It is believed
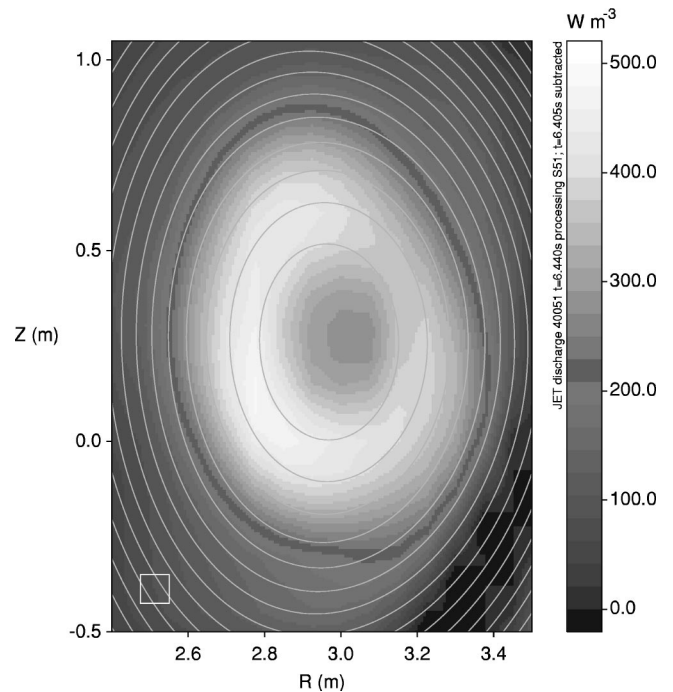

FIG. 9. Tomographic reconstruction (background subtracted) for the nickel injection in the rf heated plasma at 35 ms after the nickel injection.
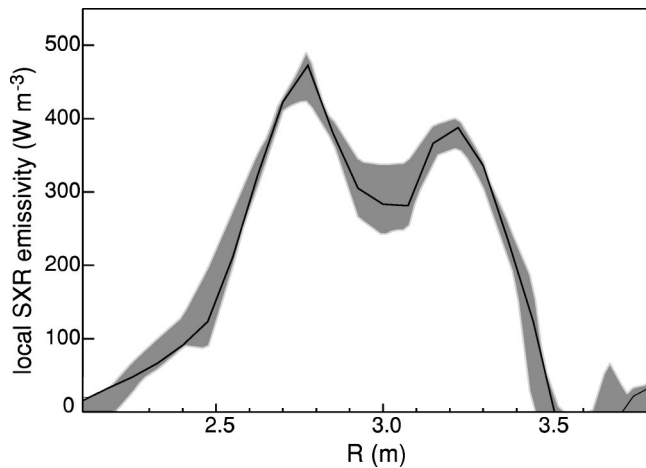
FIG. 10. Soft x-ray emissivity in the middle plane, and the gray area represents the uncertainty from the tomographic reconstruction.

FIG. 11. Perturbation to neoclassical density by the nickel poloidal rotation.

that this is the first time that this type of poloidal asymmetry was observed in a tokamak plasma.

The detailed technique involving the tomographic analysis has been reported by Ingesson *et al.*,[15] which confirms that the in–out asymmetry is above the level of uncertainty, and it is unlikely to be an artifact of the reconstruction. Figure 10 shows the background-subtracted emission in horizontal cross section of the plasma. The gray area indicates the uncertainty from the reconstruction.

Rozhansky *et al.*[8] have predicted that poloidal asymmetry should appear in the main ion density distribution in a fast poloidally rotating plasma. It is predicted[8] that the perturbation within a magnetic surface could be of the order of $\epsilon = r/R$. It was shown that for high Z impurities in the Pfirsch–Schlüter regime and main ions in the plateau regime, the poloidal variation of impurity density could be estimated as

$$\frac{n_1}{n_0} = -2\epsilon \cos\theta \left(1 - \frac{2\eta_i}{1+1.5\eta_i} \right),$$

where $\eta_i = d \ln T_i/d \ln n$ and ion poloidal rotation is the neoclassical prediction, $v_\theta = v_\theta^{\text{neo}}$.

The above-mentioned equation is in qualitative agreement with the observation of in–out asymmetric nickel density. The maximum perturbation in the midplane on the inboard side of this discharge is calculated by assuming that the T_i profile is the same as the T_e and the n_e profile the same as n_i (n_i profiles could not be measured by CXS since there were no neutral beams). The profile of the impurity ion density is shown in Fig. 11.

The peak coincides with the position where the asymmetry is observed in the experiment corresponding to the peak of the ratio $\eta_i = d \ln T_i/d \ln n$, which in neoclassical theory indicates a peak of poloidal rotation velocity. It should be noted that the soft x-ray emission is weak toward the plasma edge and some significant features in the nickel density could be missed in the tomographic reconstruction. The density perturbation on the outboard side is negative from the above equation, and these two effects give about 4%–6% difference in the density distribution. Quantitatively, the calculated
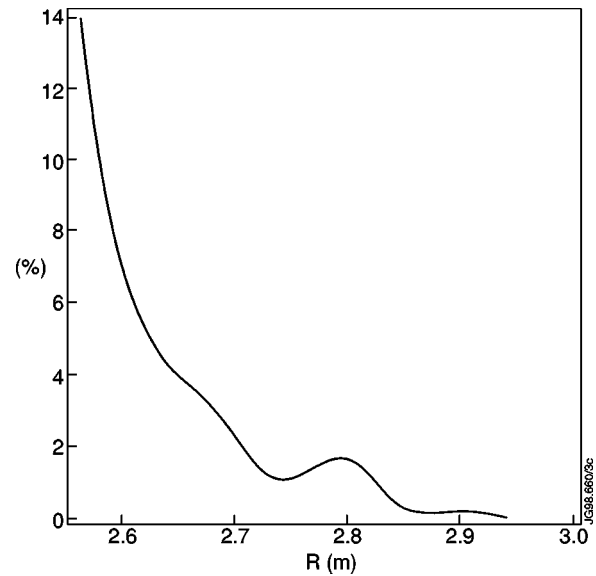
density perturbation is about a factor of 3–4 lower than that shown in tomographic reconstruction ($\sim$15%–20%).

Another theory that includes the in–out impurity asymmetry is developed by Helander.[6] It states that when the usual expansion parameter, the ratio between the ion poloidal gyroradius ρ and the radial scale length associated with the plasma density and temperature profiles, is large then poloidal asymmetries become possible. However, an estimate of the perturbation of the impurity density using the formula derived from this theory results in a density perturbation of the order of 10^{-7}. This extended neoclassical theory for steeper pressure gradients seems to predict too small a density perturbation, and therefore cannot explain the observed density asymmetry.

It should be noted that the nickel impurity asymmetry relative to the rf heating has been investigated and reported elsewhere.[15] It shows that the rf induced increase of the hydrogen-minority density on the outboard of the plasma may have resulted in the increase of the nickel density on the inboard of the plasma.

V. CONCLUSIONS

Poloidal in–out asymmetric impurity distributions have been observed experimentally in both neutral beam heated and radio frequency heated plasmas. The asymmetries in the two cases are in opposite direction. It is found that the asymmetries in the NBI heated plasmas can be explained by accounting for the centrifugal force, arising from the fast toroidal rotation, in the equilibrium ion distribution. Toroidal rotation is also related to the hollow profiles of the light impurities that have often been observed in unbalanced NBI heating plasmas. For the inboard asymmetric distribution of nickel ions observed in the rf heated plasma, the predicted ion perturbations from two sets of theories appear to be too small to explain the experimental data.

4572   Phys. Plasmas, Vol. 7, No. 11, November 2000

Chen *et al.*

[1] F. L. Hinton and S. K. Wong, Phys. Fluids **28**, 3082 (1985).
[2] W. M. Stacey and D. J. Sigmar, Phys. Fluids **28**, 2800 (1985).
[3] W. Feneberg, Nucl. Fusion **29**, 117 (1989).
[4] C. T. Hsu and D. J. Sigmar, Plasma Phys. Controlled Fusion **32**, 499 (1990).
[5] J. A. Wesson, Nucl. Fusion **37**, 557 (1997).
[6] P. Helander, Phys. Plasmas **5**, 3999 (1998).
[7] M. Romanelli and M. Ottaviani, Plasma Phys. Controlled Fusion **40**, 1767 (1998).
[8] V. Rozhansky and M. Tendler, *Reviews of Plasma Physics* (Consultants Bureau, New York, 1997), Vol. 17, p. 216.
[9] M. Tendler, Plasma Phys. Controlled Fusion **39**, B371 (1997).
[10] J. P. Smeulders, Nucl. Fusion **26**, 267 (1986).
[11] R. Dux, A. G. Peeters, A. Kallenbach, R. Neu, and the ASDEX Upgrade Team, *Proceedings of the 26th EPS Conference, Maastricht, 1999* (European Physical Society, Petit-Lancy, 1999), Europhysics Conference Abstracts Vol. 23J, p. 1409.
[12] R. Giannella, N. C. Hawkes, L. L. Taroni, M. Mattioli, J. Orourke, and D. Pasini, Plasma Phys. Controlled Fusion **34**, 687 (1992).
[13] B. Alper, A. W. Edwards, R. D. Gill, L. C. Ingesson, and M. Romanelli, *Proceedings of the 23rd EPS Conference, Kiev, 1996*, edited by R. Pick (European Physical Society, Petit-Lancy, 1996), Part I, p. a-52.
[14] JET Team (presented by C. Gormezano), *16th IAEA Fusion Energy Conference, Proceeding, Canada* (International Atomic Energy Agency, Vienna, 1997), IAEA-CN-64/A5-5, Vol. 1, p. 487.
[15] L. C. Ingesson, H. Chen, P. Helander, and M. J. Mantsinen, Plasma Phys. Controlled Fusion **42**, 161 (2000).
[16] J. L. Terry, E. S. Marmar, K. I. Chen, and H. W. Moos, Phys. Rev. Lett. **39**, 1615 (1977).
[17] K. Brau, S. Suckewer, and S. K. Wong, Nucl. Fusion **23**, 1657 (1983).
[18] L. C. Ingesson, B. Alper, H. Chen, A. W. Edwards, G. C. Fehmers, J. C. Fuchs, R. Giannella, R. D. Gill, L. Lauro-Taroni, and M. Romanelli, Nucl. Fusion **38**, 1675 (1998).
[19] M. von Hellermann (private communication).